

## Stopped-Flow Kinetics Investigation of the Imidazole-Catalyzed Peroxyoxalate Chemiluminescence Reaction

Andrew G. Hadd, Alex L. Robinson, Kathy L. Rowlen, and John W. Birks\*

Department of Chemistry and Biochemistry and Cooperative Institute for Research in Environmental Sciences (CIRES), Campus Box 216, University of Colorado, Boulder, Colorado 80309-0216

Received December 5, 1997

The stopped-flow technique was used to study the temperature-dependent kinetics of the imidazole-catalyzed peroxyoxalate reaction in order to further elucidate the reaction mechanism. Pseudo-first-order rate constants were obtained from the chemiluminescence intensity vs time profiles for the sequential reaction model  $X \rightarrow Y \rightarrow Z$  over a wide range of initial concentrations of each of the following reagents: bis(2,4,6-trichlorophenyl) oxalate (TCPO), imidazole (ImH), and hydrogen peroxide. These measurements were complemented by UV absorbance measurements of the kinetics of the step  $X \rightarrow Y$ . For both reaction conditions pseudo-first-order in TCPO ( $[ImH], [H_2O_2] \gg [TCPO]$ ) and pseudo-first-order in  $H_2O_2$  ( $[ImH] \gg [TCPO] \gg [H_2O_2]$ ), the first step of the reaction is nucleophilic substitution by two imidazole molecules to form 1,1'-oxalyldiimidazole (ODI). Under conditions of excess TCPO in the concentration range 0.075–0.25 mM, the  $Y \rightarrow Z$  reaction probed the subsequent reaction of ODI with  $H_2O_2$  to form the imidazolyl peracid intermediate, ImC(O)C(O)OOH. For excess  $H_2O_2$  concentrations in the range 2.5–15 mM, the reaction of  $H_2O_2$  with ODI is fast, and the  $Y \rightarrow Z$  step of the sequential reaction model describes subsequent reactions of the imidazolyl peracid. An important unexpected finding necessary for interpreting the kinetics of this reaction is that under conditions of a large excess of  $H_2O_2$  the faster rise of the chemiluminescence signal corresponds to the second step of the reaction ( $Y \rightarrow Z$ ), and the slower fall of the signal corresponds to the first step ( $X \rightarrow Y$ ). Lutidine and collidine, amine bases of similar aqueous  $pK_a$  as imidazole, displayed very little catalytic effect on the PO-CL reaction in comparison to imidazole, corroborating the conclusion that nucleophilic catalysis with formation of ODI as an intermediate constitutes the principal reaction pathway under conditions of both excess oxalate ester and excess  $H_2O_2$ . Imidazole quenches the quantum yield of the reaction, a result that can be well explained by catalysis of the decomposition of the key energy-transfer intermediate.

### Introduction

Although the peroxyoxalate chemiluminescence reaction has been successfully used for selective and sensitive detection of trace analytes,<sup>1–3</sup> the mechanism and identity of the intermediate(s) responsible for the chemiluminescence have not been completely elucidated.<sup>4–10</sup> Peroxyoxalate chemiluminescence (PO-CL) is described by the reaction of an aryl oxalate ester with hydrogen peroxide in the presence of a fluorophor to generate light. Optimizing PO-CL for analytical detection relies on an adequate model for the dependence of the reaction

kinetics and quantum yield on each of the reagents.<sup>11</sup> Therefore, further understanding of the reaction mechanism may improve the limits of detection and lead to the development of new chemiluminescence systems.

Although never isolated despite several kinetics and mechanistic studies, 1,2-dioxetanedione (**I**) has frequently been suggested to be the key intermediate in the PO-CL reaction.<sup>10,12,13</sup>



Kinetics studies by Catherall et al. suggest that the intermediate contains an aryl group (**II**),<sup>5</sup> and Milofsky and Birks have proposed the formation of a six-membered intermediate (**III**) on the basis of their analysis of the photoinitiated PO-CL reaction in which reaction conditions are pseudo-first-order in oxalate ester.<sup>7</sup>

Alvarez et al. proposed that multiple intermediates were capable of generating the observed light in the PO-CL reaction and that formation of different intermediates was dependent on the concentration and nature of the catalyst.<sup>6</sup>

(1) Robards, K.; Worsfold, P. J. *Anal. Chim. Acta* **1992**, *266*, 147–173.

(2) Hadd, A. G.; Birks, J. W. In *Selective Detectors: Environmental, Industrial, and Biomedical Applications*; Sievers, R. E., Ed.; John Wiley and Sons: New York, 1995; Vol. 131, pp 209–239.

(3) Bowie, A. R.; Sanders, M. G.; Worsfold, P. J. *J. Biolumin. Chemilumin.* **1996**, *11*, 61–90.

(4) Catherall, C. L.; Palmer, T. F.; Cundall, R. B. *J. Chem. Soc., Faraday Trans. 2* **1984**, *80*, 837–849.

(5) Catherall, C. L. R.; Palmer, T. F.; Cundall, R. B. *J. Chem. Soc., Faraday Trans. 2* **1984**, *80*, 823–834.

(6) Alvarez, F. J.; Parekh, N. J.; Matuszewski, B.; Givens, R. S.; Higuchi, T.; Schowen, R. L. *J. Am. Chem. Soc.* **1986**, *108*, 6435–6437.

(7) Milofsky, R. E.; Birks, J. W. *J. Am. Chem. Soc.* **1991**, *113*, 9715–9723.

(8) Orlovic, M.; Schowen, R. L.; Givens, R. S.; Alvarez, F.; Matuszewski, B.; Parekh, N. *J. Org. Chem.* **1989**, *54*, 3605.

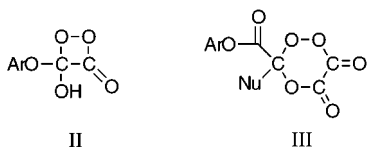
(9) Lee, J. H.; Lee, S. Y.; Kim, K.-J. *Anal. Chim. Acta* **1996**, *329*, 117–126.

(10) Stevani, C. V.; Lima, K. F.; Toscano, V. G.; Baader, W. J. *J. Chem. Soc., Perkin Trans. 2* **1996**, 989–995.

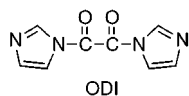
(11) Orosz, G.; Givens, R. S.; Schowen, R. L. *Crit. Rev. Anal. Chem.* **1996**, *26*, 1–27.

(12) Rauhut, M. M.; Bollyky, L. J.; Roberts, B. G.; Loy, M.; Whitman, R. H.; Iannotta, A. V.; Semsel, A. M.; Clarke, R. A. *J. Am. Chem. Soc.* **1967**, *89*, 6515–6522.

(13) Bollyky, L. J.; Whitman, R. H.; Roberts, B. G.; Rauhut, M. M. *J. Am. Chem. Soc.* **1967**, *89*, 6523–6526.



Hanaoka et al. compared different catalysts for the PO-CL reaction and found that imidazole (ImH), relative to other amine bases, had the greatest effect on the chemiluminescence yield and kinetics.<sup>14</sup> The catalytic effect of imidazole greatly exceeds predictions based solely on its basicity and has been attributed to a combination of nucleophilic and general-base catalysis.<sup>8</sup> Recently, other researchers have suggested that the predominant role of imidazole in the PO-CL reaction is as a nucleophilic catalyst, with formation of 1,1'-oxalyldiimidazole (ODI) as the main precursor in the PO-CL reaction.<sup>10,15-17</sup>



We have studied the kinetics of ODI formation in the reaction of imidazole with two oxalate esters<sup>18</sup> and the chemiluminescence reaction of ODI with hydrogen peroxide in the presence of a fluorophor<sup>19</sup> in order to clarify the role of imidazole catalysis in PO-CL. The rate-determining step in the formation of ODI from nucleophilic substitution of imidazole with bis(2,4,6-trichlorophenyl) oxalate (TCPO) and bis(2,4-dinitrophenyl) oxalate (DNPO) was found to be dependent on the structure and nonaqueous  $pK_a$  of the phenol leaving group. For TCPO, the rate-determining step was found to be expulsion of 2,4,6-trichlorophenol (TCP); substitution of the second phenol with imidazole is much faster than the first. For DNPO, addition of imidazole to a carbonyl is the rate-limiting step. The reaction of ODI with hydrogen peroxide in the presence of a fluorophor generates light in a reaction analogous to PO-CL. Because some discrepancy exists as to the number and nature of the reactive intermediates and the catalytic role of imidazole, we have investigated the kinetics of the PO-CL reaction using the stopped-flow technique over a wide range of relative reactant concentrations. To simplify the kinetics, all experiments were carried out under pseudo-first-order reaction conditions with either  $H_2O_2$  in large excess over TCPO or TCPO in large excess over  $H_2O_2$ . Also, ImH was always in large excess over TCPO.

We report for the first time the temperature-dependent kinetics of the PO-CL reaction using reaction conditions pseudo-first-order in both the oxalate ester (TCPO) and hydrogen peroxide. The effects of each of the chemiluminescence reagents on the reaction kinetics and on the relative chemiluminescence quantum yield were determined. The reaction was evaluated using imidazole, sodium salicylate, lutidine, and collidine as catalysts in order to establish the unique catalytic role of imidazole. The initial steps of the reaction were determined by

comparing the time course of the chemiluminescence emission with changes in the UV absorbance spectrum for the reactants and products. All of the results obtained are shown to be consistent with the hypothesis<sup>10,15-17</sup> that the imidazole-catalyzed peroxyoxalate reaction proceeds through the intermediate ODI.

## Experimental Section

**Chemicals.** Bis(2,4,6-trichlorophenyl) oxalate, imidazole, sodium salicylate, 2,6-dimethylpyridine (lutidine), 2,4,6-trimethylpyridine (collidine), and 9,10-diphenylanthracene (DPA) were obtained from Aldrich. Hydrogen peroxide (30% in water), obtained from Mallinckrodt, was titrated with a standardized sodium thiosulfate solution to determine the exact concentration prior to dilution. All other chemicals and solvents were used without further purification. HPLC-grade ethyl acetate (Fischer) was the solvent in all experiments. Reaction mixtures contained small amounts of water originating in the stock solution of  $H_2O_2$ .

**UV Absorbance Measurements in the Absence of a Fluorophor.** A Cary 1E UV/vis spectrophotometer was used to measure the absorbance of 2,4,6-trichlorophenol at 290 nm formed in the reaction of TCPO and imidazole. In a typical experiment, 0.5 mL of 0.20 mM TCPO in ethyl acetate from one syringe was mixed with 0.50 mL of 10.0 mM imidazole in ethyl acetate from another syringe by manually plunging the contents of both syringes into a 1.2-mL cuvette placed in the sample housing of the spectrophotometer. Reported rate constants were derived from a minimum of three measurements using a nonlinear least-squares fit to a single-exponential rise expression.<sup>20</sup>

**Chemiluminescence Measurements.** Stopped-flow chemiluminescence measurements were made using an Applied Photophysics DX-17M stopped-flow spectrophotometer (Applied Photophysics, Leatherhead, U.K.), thermostated with a Neslab RTE-110 cooler. Stock solutions of 2.0 mM TCPO, 2.0 mM DPA, 0.10 M imidazole, and 0.10 M hydrogen peroxide were prepared in ethyl acetate, stored in the dark, and remade weekly. In a typical experiment, a solution containing 0.20 mM TCPO and 0.20 mM DPA was prepared and added to one syringe of the stopped-flow instrument. Mixtures of hydrogen peroxide, 10 mM, and imidazole, 5.0–40 mM, were added to the other syringe. The reagents were mixed and profiles of chemiluminescence intensity versus time obtained after 1.5 ms. To enhance the signal-to-noise ratio, no wavelength discrimination was used when following the emission of DPA. Tabulated rate constants reflect the final post-mixing concentration. The chemiluminescence profile area, when ratioed to the initial concentration of the limiting reagent, is directly proportional to the quantum yield of the reaction. Profile areas, which are proportional to chemiluminescence quantum yields, were used to evaluate the relative effect of different reagents on the formation of light-generating intermediates. Our areas are relative to an arbitrary value of 1000 for the most intense chemiluminescence profile obtained (an entry in Table 2). Very little additional mechanistic insight would be provided by absolute quantum yields.

**Analysis of Rate Data.** The kinetics of each profile was analyzed using a sequential-reaction model<sup>7,8</sup>



where X represents reactants; Y, intermediates; and Z, products; and  $k_1$  and  $k_2$  are pseudo-first-order rate constants. Using this model, the chemiluminescence intensity is proportional to the concentration of species Y, and both reaction steps are first-order, irreversible reactions. The integrated rate law describes the combined exponential contribution of the two rate constants to the observed signal intensity,  $I$ , at any time,  $t$ ,

(14) Hanaoka, N.; Givens, R. S.; Schowen, R. L.; Kuwana, T. *Anal. Chem.* **1988**, *60*, 2193-2197.

(15) Neuvonen, H. *J. Chem. Soc., Perkin Trans. 2* **1995**, 945.

(16) Stigbrand, M.; Ponten, E.; Irgum, K. *Anal. Chem.* **1994**, *66*, 1766.

(17) Emteborg, M.; Ponten, E.; Irgum, K. *Anal. Chem.* **1997**, *69*, 2109-2114.

(18) Hadd, A. G.; Birks, J. W. *J. Org. Chem.* **1996**, *61*, 2657-2663.

(19) Hadd, A. G.; Seeber, A.; Birks, J. W. Manuscript in preparation.

(20) Espenson, J. H. *Chemical Kinetics and Reaction Mechanisms*; McGraw-Hill: New York, 1981.

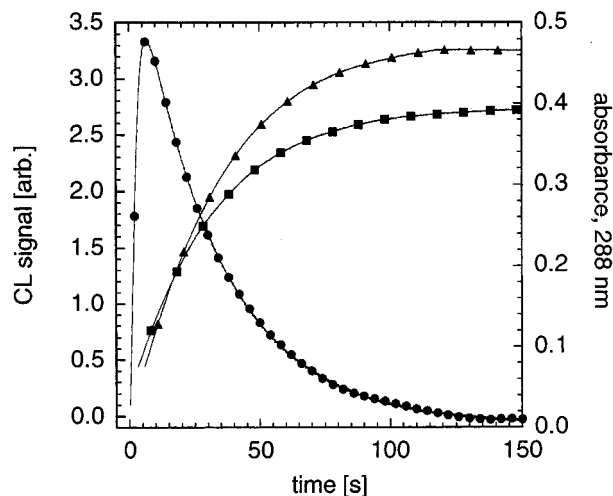


**Figure 1.** Plot comparing chemiluminescence intensity of the PO-CL reaction with the UV absorbance of 2,4,6-trichlorophenol vs time in the reaction of 0.10 mM TCPO and 5.0 mM imidazole. The chemiluminescence intensity (●), left axis, was measured by adding 0.10 mM DPA and 5.0 mM H<sub>2</sub>O<sub>2</sub>. UV absorbance is shown on the right axis for the reaction without hydrogen peroxide (▲), and with 5.0 mM H<sub>2</sub>O<sub>2</sub> (■).

where  $M$  is the maximum intensity. Equation 2 may be fit

$$I = \frac{MK_1}{K_2 - K_1} (e^{-K_2 t} - e^{-K_1 t}) \quad (2)$$

equally well by two expressions in which  $K_1$  and  $K_2$  are interchanged.<sup>10,19,20</sup> A unique solution requires an independent method of measuring  $K_1$  or  $K_2$ . As discussed in the Results, this was accomplished in separate experiments in which the appearance of the product 2,4,6-trichlorophenol was monitored by UV absorbance. Pseudo-first-order rate constants were derived from a nonlinear least-squares fit to eq 2 using the software Kaleidagraph. Reported rate constants are an average of at least three independent measurements and were determined by nonlinear regression fits to a minimum of 500 data points.

## Results and Discussion

**Comparison of Rate Constants Derived from UV Absorbance and Chemiluminescence Measurements.** The reaction of TCPO and imidazole with or without hydrogen peroxide produced 2,4,6-trichlorophenol, monitored at its maximum absorbance at 290 nm. This reaction was studied over the imidazole concentration range of 2.5–15.0 mM with and without 5.0 mM H<sub>2</sub>O<sub>2</sub>. In Figure 1, the absorbance of TCP versus time produced in the reaction of 0.10 mM TCPO with 5.0 mM imidazole with and without H<sub>2</sub>O<sub>2</sub> (right axis) is compared to a chemiluminescence signal profile (left axis). The chemiluminescence signal was obtained by detecting the emitted light from diphenylanthracene (DPA) added to the reaction of 0.10 mM TCPO, 5.0 mM ImH, and 5.0 mM H<sub>2</sub>O<sub>2</sub>.

The two reactions monitored by UV absorbance at 290 nm, one with and one without 5.0 mM H<sub>2</sub>O<sub>2</sub>, have similar absorbance profiles and rate constants. The time course of the absorbance increase follows a single-exponential rise for both reactions with an average rate constant of  $3.08(\pm 0.07) \times 10^{-2} \text{ s}^{-1}$ , and the final absorbance corresponds to the release of both phenols from TCPO. Without hydrogen peroxide, a stable product other than

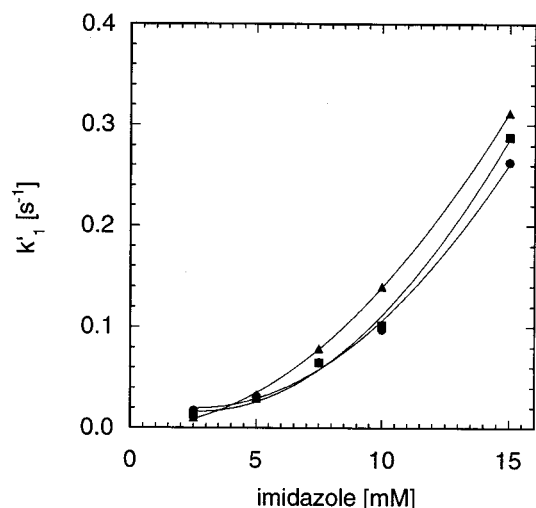


**Figure 2.** Effect of imidazole concentration on  $K_1$  for the PO-CL reaction measured by chemiluminescence (●), and the reaction of 0.10 mM TCPO with imidazole without H<sub>2</sub>O<sub>2</sub> (▲) and with 5.0 mM H<sub>2</sub>O<sub>2</sub> (■) measured by UV absorbance of 2,4,6-trichlorophenol at 290 nm.

TCP is formed, contributing to the higher final absorbance at 290 nm. On the basis of our previous study of the kinetics of the reaction of TCPO with ImH, this product is ODI.<sup>18</sup> The CL signal follows rise-fall kinetics (eq 1) with a fast increase in the signal followed by a slower decrease. A nonlinear least-squares fit of the CL profile to eq 2 produced two rate constants,  $3.30(\pm 0.01) \times 10^{-1} \text{ s}^{-1}$  for the rapid increase of the CL signal and  $3.61(\pm 0.01) \times 10^{-2} \text{ s}^{-1}$  for the slower decay. Thus, the pseudo-first-order rate constant for the signal decay is in good agreement with the rate constant for formation of TCP as measured by UV absorption.

As seen in Figure 2, the rate constants from the reactions monitored by UV absorbance (with and without 5.0 mM H<sub>2</sub>O<sub>2</sub>) and the rate constant derived from decay of the CL signal all have a second-order dependence on the imidazole concentration. This result, combined with the good agreement between the rate coefficients obtained for the production of TCP (and ODI) and the slow decline of the CL signal, indicates that the slow step of the chemiluminescent reaction corresponds to the double substitution reaction of ImH with TCPO to form ODI. Thus, the pseudo-first-order rate constant  $K_1$  corresponds to the slow decay of the CL signal, and  $K_2$  corresponds to the fast rise for conditions of  $[\text{ImH}], [\text{H}_2\text{O}_2] \gg [\text{TCPO}]$ .

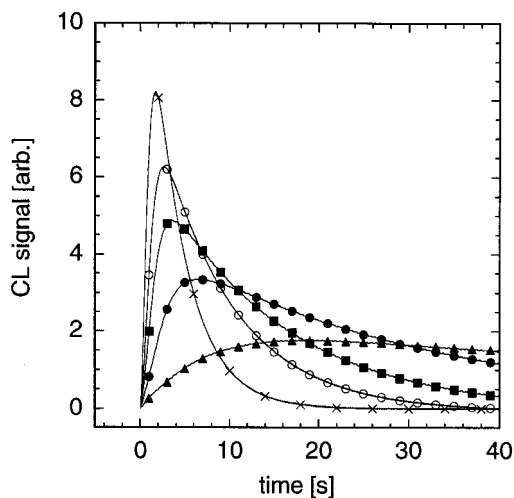
**PO-CL Reaction Evaluated Using Conditions of a Large Excess of H<sub>2</sub>O<sub>2</sub> Effect of the TCPO Concentration.** The TCPO concentration was varied in the range 0.075–0.25 mM in reactions with 5.0 mM H<sub>2</sub>O<sub>2</sub> and 10.0 mM ImH. The derived rate constants,  $K_1$  and  $K_2$ , and the profile areas are summarized in Table 1. Within experimental error, both  $K_1$  and  $K_2$  are independent of the TCPO concentration, confirming that, under these conditions, the reaction is pseudo-first order in TCPO. Over a 3.3-fold increase in the TCPO concentration, the profile area increased linearly by 3.5-fold. This result is consistent with TCPO being the limiting reagent under these reaction conditions.

**Effect of Imidazole Concentration and Temperature.** The effect of increasing the imidazole concentration from 2.5 to 20.0 mM on the PO-CL reaction was evaluated in the temperature range 6–45 °C. For a given

**Table 1.** Effect of TCPO Concentration on  $k_1$ ,  $k_2$ , and Profile Area with  $\text{H}_2\text{O}_2$  in Large Excess over TCPO<sup>a</sup>

TCPO, mM	$k_1$ , s <sup>-1</sup>	$k_2$ s <sup>-1</sup>	area, au
0.075	0.141 ± 0.002	1.73 ± 0.01	175 ± 10
0.10	0.123 ± 0.002	2.52 ± 0.04	280 ± 15
0.15	0.126 ± 0.002	1.48 ± 0.02	360 ± 20
0.20	0.123 ± 0.002	1.45 ± 0.02	485 ± 25
0.25	0.098 ± 0.003	2.23 ± 0.08	610 ± 30

<sup>a</sup> Reaction conditions: 5.0 mM  $\text{H}_2\text{O}_2$ , 10.0 mM ImH, 0.10 mM DPA, 25 °C.

**Figure 3.** Effect of imidazole concentration on the chemiluminescence signal vs time profile. Conditions: (▲) 2.5 mM, (●) 5.0 mM, (■) 7.5 mM, (○) 10.0 mM, and (×) 15.0 mM imidazole with 5.0 mM  $\text{H}_2\text{O}_2$ , 0.10 mM TCPO, and 0.10 mM DPA at 25 °C.**Table 2.** Effect of Imidazole Concentration on  $k_1$ ,  $k_2$ , and Profile Area with  $\text{H}_2\text{O}_2$  in Large Excess over TCPO<sup>a</sup>

[imidazole], mM	$10^2 k_1$ , s <sup>-1</sup>	$k_2$ , s <sup>-1</sup>	area, au
2.50	1.04 ± 0.01	0.148 ± 0.001	1,000 ± 50
3.50	1.99 ± 0.02	0.232 ± 0.001	875 ± 45
5.00	3.61 ± 0.01	0.330 ± 0.001	650 ± 35
7.50	7.98 ± 0.02	0.534 ± 0.006	445 ± 25
10.0	13.7 ± 0.1	0.66 ± 0.01	370 ± 20
15.0	32.2 ± 0.2	0.84 ± 0.02	195 ± 10
20.0	58 ± 2	0.84 ± 0.04	185 ± 10

<sup>a</sup> Reaction conditions: 5.0 mM  $\text{H}_2\text{O}_2$ , 0.10 mM TCPO, 0.10 mM DPA, 25 °C.

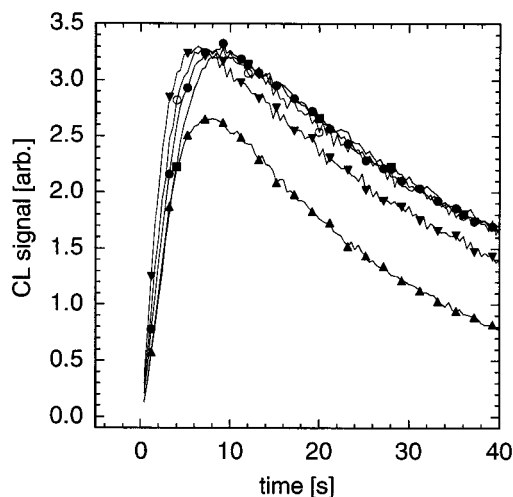
temperature, as the ImH concentration increased, the maximum signal intensity increased, and the time to reach the maximum signal decreased, as seen in Figure 3 for a temperature of 25 °C. The profile area decreased 6-fold, however, as the imidazole concentration was increased from 2.5 to 20.0 mM. A plot of the profile area vs  $[\text{ImH}]^{-1}$  produces a straight line having a correlation coefficient of  $r^2 = 0.998$ . At each temperature, the profiles were similar in shape, and, for a given ImH concentration, the profile area increased with temperature. The calculated pseudo-first-order rate constants and the profile areas obtained at 25 °C are summarized in Table 2. At each temperature, the rate constant  $k_1$  displayed a second-order dependence on the imidazole concentration (Figure 2). Terms in the fitted equation

$$k_1 = k_{1a} + k_{1b}[\text{ImH}] + k_{1c}[\text{ImH}]^2 \approx k_{1c}[\text{ImH}]^2 \quad (3)$$

were dominated by the second-order component,  $k_{1c}[\text{ImH}]^2$ . The rate constant,  $k_2$ , increased linearly with imidazole

**Table 3.** Effect of Temperature on the Derived Third-Order Rate Constant for  $k_c$  and Second-Order Rate Constant for  $k_{2b}$  with  $\text{H}_2\text{O}_2$  in Large Excess over TCPO

$T$ , °C	$k_{1c}$ , M <sup>-2</sup> s <sup>-1</sup>	$k_{2b}$ , M <sup>-1</sup> s <sup>-1</sup>
6	1900 ± 200	41 ± 5
15	1420 ± 20	49 ± 7
25	1600 ± 150	75 ± 5
35	1430 ± 10	120 ± 4
45	1200 ± 80	130 ± 4

**Figure 4.** Effect of hydrogen peroxide concentration on the chemiluminescence signal vs time profile. Conditions: (▲) 2.5 mM, (●) 5.0 mM, (■) 7.5 mM, (○) 10.0 mM, and (▼) 15.0 mM hydrogen peroxide with 5.0 mM imidazole, 0.10 mM TCPO, and 0.10 mM DPA at 25 °C.

concentration below 10.0 mM but leveled off at higher concentrations, reaching a maximum of  $0.98 \pm 0.02$  s<sup>-1</sup> at 20.0 mM ImH. A plot of  $k_2$  vs  $[\text{ImH}]$  evaluated in the linear range passed through the origin within experimental error, the slope of which produces a second-order rate constant. Values at each temperature for the third-order rate constant for reaction  $k_{1c}$  and the second-order rate constant for  $k_{2b}$  (where  $k_2 = k_{2a} + k_{2b}[\text{ImH}]$ ) are summarized in Table 3. The rate constant  $k_{1c}$  has a small negative activation energy of  $-7 \pm 3$  kJ mol<sup>-1</sup> ( $\Delta S^\ddagger = 38 \pm 8$  J K<sup>-1</sup> mol<sup>-1</sup>,  $r^2 = 0.71$ ), whereas an activation energy of  $24 \pm 3$  kJ mol<sup>-1</sup> ( $\Delta S^\ddagger = 117 \pm 9$  J K<sup>-1</sup> mol<sup>-1</sup>,  $r^2 = 0.96$ ) is calculated from an Arrhenius plot for  $k_{2b}$ .

The second-order dependence of  $k_1$  on ImH concentration is consistent with the hypothesis that the first step of the reaction is ImH catalysis of nucleophilic substitution of ImH to form ODI from TCPO. The first-order dependence of  $k_2$  on ImH concentration at low ImH concentrations is consistent with base catalysis by ImH of a subsequent reaction.

**Effect of Hydrogen Peroxide Concentration.** The chemiluminescence profiles obtained by varying the large excess of hydrogen peroxide concentration in the range 2.5–15.0 mM are shown in Figure 4, and the derived pseudo-first-order rate constants and profile areas are summarized in Table 4. The area increased significantly, from  $460 \pm 25$  to  $920 \pm 45$  arbitrary units (au), in the  $\text{H}_2\text{O}_2$  concentration range of 2.5–5.0 mM, remained constant at  $920 \pm 45$  au in the range 5.0 to 10.0 mM, and decreased slightly to  $810 \pm 40$  au at 15.0 mM. In the concentration range 5–15 mM,  $k_1$  was independent of  $\text{H}_2\text{O}_2$  concentration. This was confirmed by monitoring the formation of TCP by UV absorbance; increasing the

**Table 4. Effect of Hydrogen Peroxide on  $K_1$ ,  $K_2$ , and Profile Area with  $H_2O_2$  in Large Excess over TCPO<sup>a</sup>**

[H <sub>2</sub> O <sub>2</sub> ], mM	10 <sup>2</sup> $K_1$ , s <sup>-1</sup>	$K_2$ , s <sup>-1</sup>	area, au
2.50	4.45 ± 0.02	0.249 ± 0.004	460 ± 25
5.00	2.62 ± 0.02	0.217 ± 0.004	920 ± 45
7.50	2.34 ± 0.02	0.286 ± 0.004	920 ± 45
10.0	2.35 ± 0.02	0.327 ± 0.004	920 ± 45
15.0	2.70 ± 0.02	0.421 ± 0.005	810 ± 40

<sup>a</sup> Reaction conditions: 5.0 mM ImH, 0.10 mM TCPO, 0.10 mM DPA, 25 °C.

H<sub>2</sub>O<sub>2</sub> concentration from 2.5 to 15.0 mM in the reaction of 5.0 mM ImH with 0.10 mM TCPO had no significant effect on the pseudo-first-order rate constant  $K_1$ . Ignoring the data at 2.5 mM H<sub>2</sub>O<sub>2</sub>, which appear to be anomalous (see Figure 4; a possible explanation for this anomaly is given below), the average value of  $K_1$  is  $2.5(\pm 0.2) \times 10^{-2}$  s<sup>-1</sup>. At 45 mM H<sub>2</sub>O<sub>2</sub>, however, an increase to  $5.7(\pm 0.1) \times 10^{-2}$  s<sup>-1</sup> for  $K_1$  was observed. The lack of dependence of  $K_1$  on excess H<sub>2</sub>O<sub>2</sub> concentration in the range 5–15 mM H<sub>2</sub>O<sub>2</sub> is consistent with the first step of the reaction being the double ImH substitution to form ODI from TCPO. One possible explanation for the increased value of  $K_1$  at very high H<sub>2</sub>O<sub>2</sub> concentration is an additional reaction of the singly substituted TCPO molecule with H<sub>2</sub>O<sub>2</sub> to form the corresponding peroxyoxalate.

With the exception of the result obtained at 2.5 mM, which again appears to be anomalous, the fall rate constant increased with increasing hydrogen peroxide concentration. A plot of  $K_2$  versus [H<sub>2</sub>O<sub>2</sub>] for all rate constants given in Table 4 has a positive intercept of  $0.18 \pm 0.04$  s<sup>-1</sup> and a slope of  $16 \pm 3$  M<sup>-1</sup> s<sup>-1</sup>. Ignoring the data point at 2.5 mM H<sub>2</sub>O<sub>2</sub>, the intercept is  $0.13 \pm 0.01$  s<sup>-1</sup> and the slope is  $20 \pm 1$  M<sup>-1</sup> s<sup>-1</sup>. The intercept represents a first-order rate constant for a reaction zero-order in hydrogen peroxide concentration, and the slope represents a second-order rate constant for a reaction first-order in hydrogen peroxide.

The first-order dependence of  $K_2$  on H<sub>2</sub>O<sub>2</sub> concentration would be consistent with the hypothesis that the second step of the reaction is substitution of H<sub>2</sub>O<sub>2</sub> for ImH in ODI. However, this would not explain the large zero-order component of the dependence of  $K_2$  on [H<sub>2</sub>O<sub>2</sub>]. It is more likely that the first substitution of ODI by H<sub>2</sub>O<sub>2</sub> is very fast ( $0.6$ – $3.9$  s<sup>-1</sup> for 2.5–15 mM H<sub>2</sub>O<sub>2</sub> in acetonitrile)<sup>19</sup> compared to the conversion of TCPO to ODI, at least at higher H<sub>2</sub>O<sub>2</sub> concentrations. This is supported by the UV absorbance experiment shown in Figure 1 in which the formation of products proceeds at the same rate in the presence and absence of 5.0 mM H<sub>2</sub>O<sub>2</sub>. Thus, the rate constant  $K_2$  must describe the fate of a product of the reaction of H<sub>2</sub>O<sub>2</sub> with ODI. As discussed below, the zero-order component could be due to the unimolecular cyclization of the intermediate imidazolyl hydroperoxide, ImC(O)C(O)OOH, to form an energy-transfer intermediate, and the first-order dependence of  $K_2$  on [H<sub>2</sub>O<sub>2</sub>] may be due to a second substitution of H<sub>2</sub>O<sub>2</sub> to form HOOC(O)C(O)OOH. The assumption that the reaction of H<sub>2</sub>O<sub>2</sub> with ODI is fast compared to the formation of ODI is consistent with the rate constant derived below for the H<sub>2</sub>O<sub>2</sub> + ODI reaction under conditions of a large excess of TCPO except in the range of 2.5–5.0 mM H<sub>2</sub>O<sub>2</sub> where the anomalous results were obtained. Thus, the anomalous effects on  $K_1$  and  $K_2$  at low H<sub>2</sub>O<sub>2</sub> may be due to the lack of a single, rate-determining step in this concentration regime.

**Table 5. Effect of Temperature on  $K_1$  and  $K_2$  for the Sodium Salicylate Catalyzed PO-CL Reaction<sup>a</sup>**

T, °C	10 <sup>3</sup> $K_1$ , s <sup>-1</sup>	$K_2$ , s <sup>-1</sup>
10	1.22 ± 0.05	0.9 ± 0.1
20	2.11 ± 0.04	4.2 ± 0.4
30	3.43 ± 0.01	4.9 ± 0.4
38	4.95 ± 0.05	8.3 ± 0.5

<sup>a</sup> Reaction conditions: 4.0 mM H<sub>2</sub>O<sub>2</sub>, 0.10 mM TCPO, 0.10 mM sodium salicylate, 0.10 mM DPA.

**Table 6. Effect of Imidazole on  $K_1$ ,  $K_2$ , and Profile Area with TCPO in Large Excess over H<sub>2</sub>O<sub>2</sub>**

[imidazole], mM	10 <sup>2</sup> $K_1$ , s <sup>-1</sup>	10 <sup>2</sup> $K_2$ , s <sup>-1</sup>	area, au
2.50	0.83 ± 0.01	0.50 ± 0.01	10.0 ± 0.5
3.50	1.66 ± 0.01	0.63 ± 0.01	12.5 ± 0.6
5.00	3.18 ± 0.02	0.95 ± 0.01	10.0 ± 0.5
7.50	6.51 ± 0.02	1.56 ± 0.02	8.3 ± 0.4
10.0	11.1 ± 0.2	2.21 ± 0.05	7.0 ± 0.4
15.0	25.0 ± 0.2	3.67 ± 0.03	4.3 ± 0.2
20.0	38.1 ± 0.2	5.40 ± 0.03	4.2 ± 0.2

<sup>a</sup> Reaction Conditions: 5.0 μM H<sub>2</sub>O<sub>2</sub>, 0.10 mM TCPO, 0.10 mM DPA, 25 °C.

**Effect of General Base Catalysts.** The PO-CL reaction was evaluated using two sterically hindered bases, lutidine and collidine, which have a similar aqueous p*K*<sub>a</sub> as imidazole. Neither base significantly catalyzed the PO-CL reaction. For equal concentrations of amine, 2% of the profile area in the imidazole-catalyzed reaction was obtained with lutidine and 0.6% with collidine. For 5.0 mM amine, the values for  $K_1$  using collidine,  $9.3 \times 10^{-4}$  s<sup>-1</sup>, and lutidine,  $1.6 \times 10^{-4}$  s<sup>-1</sup>, were, respectively, 35 and 200 times less than  $K_1$  using imidazole as the catalyst.

The PO-CL reaction catalyzed by sodium salicylate was evaluated in the 10–38 °C temperature range. In these experiments, the post-mixing reagent concentrations were 0.10 mM TCPO, 0.05 mM DPA, 4.0 mM H<sub>2</sub>O<sub>2</sub>, and 0.10 mM sodium salicylate. Rate constants,  $K_1$  for the slow signal decay, and  $K_2$ , for the rapid signal increase, were measured as a function of temperature and are given in Table 5. Arrhenius plots produce activation energies of  $36.5 \pm 0.4$  kJ mol<sup>-1</sup> ( $\Delta S^\ddagger = 188 \pm 1$  J K<sup>-1</sup> mol<sup>-1</sup>,  $r^2 = 0.9998$ ) for  $K_1$  and  $54 \pm 14$  kJ mol<sup>-1</sup> ( $\Delta S^\ddagger = 192 \pm 48$  J K<sup>-1</sup> mol<sup>-1</sup>,  $r^2 = 0.88$ ) for  $K_2$ .

**PO-CL Reaction Evaluated Using a Large Excess of TCPO (Pseudo-First-Order in H<sub>2</sub>O<sub>2</sub>).** **Effect of Temperature and Imidazole Concentration.** The PO-CL reaction was investigated using conditions in which the TCPO concentration, 0.10 mM, was in large excess over the hydrogen peroxide concentration, 5.0 μM, for imidazole concentrations in the range 2.5–15.0 mM and over the temperature range 7–45 °C. Qualitatively, the shape of each chemiluminescence profile was similar to that shown in Figure 3 with the maximum intensity increasing and time to reach maximum intensity decreasing with increasing imidazole concentration. The derived rate constants,  $K_1$  and  $K_2$ , obtained at 25 °C, along with the relative profile areas, are summarized in Table 6. Comparing the profile areas in Tables 2 and 6, it may be seen that the quantum yield of the reaction is nearly equal for both reaction conditions after correction is made for the concentration of the limiting reagent.

In contrast to pseudo-first-order TCPO conditions, when imidazole is in large excess over TCPO and both are in excess over H<sub>2</sub>O<sub>2</sub>,  $K_1$  reflects the increase of the CL signal and  $K_2$  the decrease. We infer this by compar-

ing measured rise and fall rate constants and from the dependencies of the rates on ImH concentration. The CL signal rises with a second-order dependence on the imidazole concentration; the corresponding third-order rate constant of  $1.10(\pm 0.05) \times 10^2 \text{ M}^{-2} \text{ s}^{-1}$  differs by only 30% from the value of  $1.60(\pm 0.012) \times 10^2 \text{ M}^{-2} \text{ s}^{-1}$  obtained for  $K_1$  (CL signal decline) under excess  $\text{H}_2\text{O}_2$  conditions. This agreement in rate constants is remarkable, especially considering the several orders of magnitude difference in reagent concentrations; the 30% slower reaction under excess  $\text{H}_2\text{O}_2$  conditions could be attributed to the higher concentration of water (0.6 to 3.4 mM  $\text{H}_2\text{O}$  for excess  $\text{H}_2\text{O}_2$  conditions vs 1.1  $\mu\text{M}$   $\text{H}_2\text{O}$  for excess TCPO). It is well-known that water strongly affects the kinetics and quantum yield of the peroxyoxalate reaction.<sup>2</sup> The fall of the signal is approximately first-order in ImH with only a slight second-order contribution. Thus, under conditions of excess TCPO, the reaction profile assumes the more familiar situation where the increase of the chemiluminescence signal follows the conversion of TCPO to an intermediate(s), and the decay of that intermediate is slower than its formation.

The pseudo-first-order rate constants for  $K_1$  and  $K_2$  were resolved into zero-, first-, and second-order contributions as described by eqs 4 and 5:

$$K_1 = k_{1d} + k_{1e}[\text{ImH}] + k_{1f}[\text{ImH}]^2 \quad (4)$$

$$K_2 = k_{2d} + k_{2e}[\text{ImH}] + k_{2f}[\text{ImH}]^2 \quad (5)$$

The values for  $k_{1f}$  in units of  $\text{M}^{-2} \text{ s}^{-1}$  at 7, 15, 25, 35, and 45 °C are 700, 840, 1100, 1250, and 1600  $\text{s}^{-1}$ , respectively, with an average uncertainty of 100  $\text{M}^{-2} \text{ s}^{-1}$ . The activation energy associated with the increase of  $k_{1f}$  with temperature is  $15.8 \pm 0.8 \text{ kJ mol}^{-1}$  ( $\Delta S^\ddagger = 111 \pm 3 \text{ J K}^{-1} \text{ mol}^{-1}$ ,  $r^2 = 0.992$ ).

Although showing a slight second-order dependence on imidazole concentration, the value for  $K_2$  was mainly determined by  $k_{2e}$ , the component of the reaction rate that is first-order in imidazole concentration. For  $K_2$ , the second-order dependence on the imidazole concentration was unobservable at 7 and 15 °C, and  $k_{2f}$  was only  $50 \pm 8 \text{ M}^{-2} \text{ s}^{-1}$  at 25 °C and  $88 \pm 1 \text{ M}^{-2} \text{ s}^{-1}$  at 45 °C. The values for  $k_{2e}$  at 7, 15, 25, 35, and 45 °C are 1.2, 2.0, 1.6, 1.6, and 1.2  $\text{M}^{-1} \text{ s}^{-1}$  with an average uncertainty of 0.2  $\text{M}^{-1} \text{ s}^{-1}$ . Thus, the rate constant  $k_{2e}$  is approximately independent of temperature.

The second-order dependence of  $K_1$  on ImH again is consistent with the first step of the reaction being ImH catalysis of the nucleophilic substitution of ImH into TCPO to form ODI. The predominantly first-order dependence of  $K_2$  on [ImH] is consistent with general base catalysis by ImH of a subsequent reaction.

As found for conditions of excess  $\text{H}_2\text{O}_2$ , increasing concentration of imidazole caused a decrease in profile area (see Table 6), which is proportional to the chemiluminescence quantum yield. Again, the profile area was inversely related to imidazole concentration.

**Effect of TCPO Concentration.** The TCPO concentration was varied in the range 0.075–0.25 mM in order to determine the order of the reaction with respect to TCPO. Final concentrations of 10 mM ImH and 5.0  $\mu\text{M}$   $\text{H}_2\text{O}_2$  were used for all experiments. Table 7 gives the derived values of  $K_1$  and  $K_2$  and relative profile areas. Examples of the chemiluminescence profiles along with

**Table 7. Effect of TCPO Concentration on  $K_1$ ,  $K_2$ , and Profile Area with TCPO in Large Excess over  $\text{H}_2\text{O}_2$ <sup>a</sup>**

[TCPO], mM	$K_1$ , $\text{s}^{-1}$	$K_2$ , $\text{s}^{-1}$	area, au
0.075	$0.115 \pm 0.005$	$0.018 \pm 0.005$	$15.8 \pm 0.8$
0.10	$0.121 \pm 0.003$	$0.025 \pm 0.003$	$15.0 \pm 0.8$
0.15	$0.098 \pm 0.005$	$0.048 \pm 0.004$	$10.0 \pm 0.5$
0.20	$0.115 \pm 0.008$	$0.060 \pm 0.006$	$15.8 \pm 0.8$
0.25	$0.110 \pm 0.003$	$0.081 \pm 0.003$	$11.7 \pm 0.6$

<sup>a</sup> Reaction conditions: 5.0  $\mu\text{M}$  ImH, 10.0 mM ImH, 0.10 mM DPA, 25 °C.

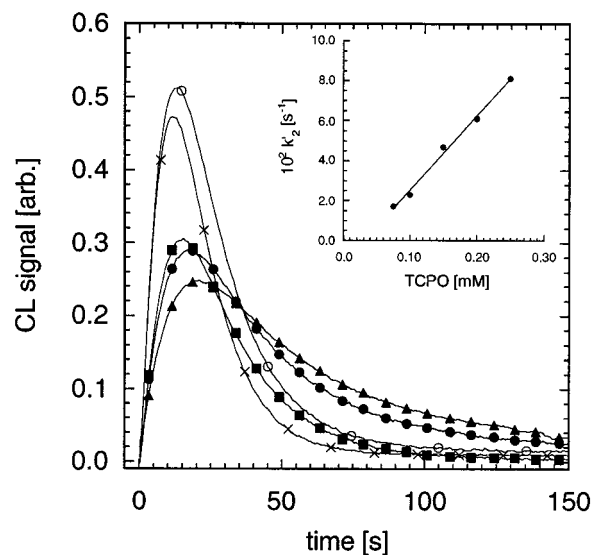


**Figure 5.** Effect of TCPO concentration on the chemiluminescence signal vs time profile and  $K_2$  (inset), with the TCPO concentration in large excess over the  $\text{H}_2\text{O}_2$  concentration. Conditions: (▲) 0.075 mM, (●) 0.10 mM, (■) 0.15 mM, (○) 0.20 mM, and (×) 0.25 mM TCPO with 10.0 mM imidazole, 5.0  $\mu\text{M}$   $\text{H}_2\text{O}_2$ , and 0.10 mM DPA at 25 °C.

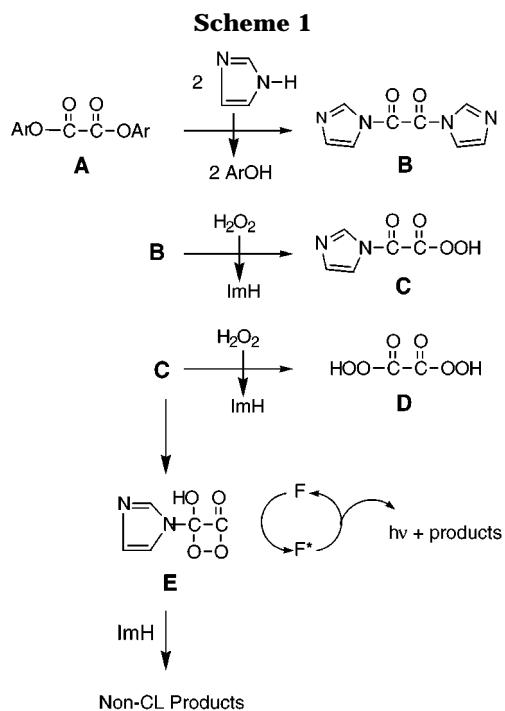
a plot of the increase in  $K_2$  with increasing TCPO concentration (inset) are shown in Figure 5. The maximum signal increased in the concentration range 0.075–0.20 mM and then began to decrease at 0.25 mM TCPO. The profile area was nearly constant at  $\sim 15$  au, decreasing to  $\sim 12$  au at 0.25 mM TCPO. The rate constant  $K_1$  was independent of the TCPO concentration, whereas a plot of  $K_2$  versus TCPO concentration (inset of Figure 5) was linear with an intercept not significantly different from zero and slope of  $3.7(\pm 0.2) \times 10^2 \text{ M}^{-1} \text{ s}^{-1}$ .

The lack of dependence of  $K_1$  on TCPO concentration confirms the establishment of pseudo-first-order conditions in TCPO with respect to its reaction with ImH and further verifies the assignment of  $k_1$  to the CL signal rise. The first-order dependence of  $K_2$  on TCPO is well explained if the second step of the reaction is the nucleophilic reaction of  $\text{H}_2\text{O}_2$  with ODI since the concentration of ODI formed in the first step is equal to the initial TCPO concentration.

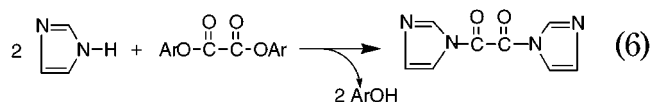
### Reaction Mechanism

A mechanism consistent with all of the kinetics observations is given in Scheme 1. Table 8 summarizes the reaction steps probed by the kinetics and the rate laws that apply to this mechanism for pseudo-first-order reaction conditions with either  $\text{H}_2\text{O}_2$  or TCPO in large excess.

**Excess  $\text{H}_2\text{O}_2$  Conditions.** All of the results are consistent with the conclusion that under conditions of



a large excess of  $\text{H}_2\text{O}_2$  and ImH over TCPO formation of ODI is the rate-limiting step for the rise reaction. The pseudo-first-order rate constant,  $k_1$ , has a second-order dependence on the ImH concentration and no dependence on the initial  $\text{H}_2\text{O}_2$  concentration, as measured either by chemiluminescence or by UV absorbance of the product TCP. In addition, the absorbance of TCP increased with one observed rate constant to a final absorbance corresponding to the production of 2 mol of phenol for every mole of TCPO. These results are consistent with the nucleophilic substitution of two molecules of imidazole into TCPO to form ODI:



The first- and second-order dependence on the imidazole concentration is characteristic of nucleophilic substitution reactions of imidazole in which substitution by imidazole is catalyzed by another molecule of imidazole.<sup>15,21–23</sup> Ester aminolysis in aprotic solvents is rate limited by the collapse of the tetrahedral intermediate.<sup>24</sup> For reactions involving imidazole, collapse of the tetrahedral intermediate is catalyzed by another molecule of imidazole, either by proton transfer from the substituted imidazole or proton transfer to the phenol leaving group.<sup>22,25,26</sup> In the PO-CL reaction, the substitution of the second imidazole to TCPO was apparently fast in comparison to the first, an observation consistent with other studies of the reaction of imidazole with oxalate esters<sup>10</sup> and our previous study of the nucleophilic

reaction of ImH with TCPO.<sup>18</sup> The accelerated addition of the second imidazole apparently results from activation of the adjacent oxalate carbonyl by the first substituted imidazole.<sup>18</sup>

ODI has a very short lifetime in the presence of excess hydrogen peroxide. As seen in Figure 1, the absorbance profile at 290 nm for the reaction of 0.10 mM TCPO and 5.0 mM ImH has the same first-order rate constant but a greater absorbance (due to the ODI product) than the same reaction with 5.0 mM  $\text{H}_2\text{O}_2$  added. The similarity of the rate constants and the lack of a rise-fall absorbance profile suggests that reaction of ODI with  $\text{H}_2\text{O}_2$  is fast relative to formation of ODI. Thus, the rise rate reaction described by  $k_1$  results in the formation of an imidazolyl peracid, species **C** of Scheme 1, a reaction step commonly proposed in other mechanistic studies of the PO-CL reaction.<sup>5,7,8,10,12</sup>

It was found that hydrogen peroxide does affect the rise rate at significantly higher concentrations. For example, at 45 mM  $\text{H}_2\text{O}_2$ ,  $k_1$  is  $5.7(\pm 0.1) \times 10^{-2} \text{ s}^{-1}$ , compared to the average  $2.5(\pm 0.2) \times 10^{-2} \text{ s}^{-1}$  in the 5 to 15 mM range. A zero-order dependence at low  $\text{H}_2\text{O}_2$  concentration with a first-order dependence at higher  $\text{H}_2\text{O}_2$  concentration has been observed previously.<sup>5,27</sup> At higher  $\text{H}_2\text{O}_2$  concentration, it is possible that  $\text{H}_2\text{O}_2$  substitutes directly into TCPO as a result of base catalysis alone to form the peroxyoxalate intermediate.

The chemiluminescence profile shapes are well explained if the signal is proportional to the formation and decay of the imidazolyl peracid, **C**. Under conditions of a large excess of  $\text{H}_2\text{O}_2$ , the decay of **C** has a complex dependence on the imidazole concentration with a zero- and first-order dependence on the hydrogen peroxide concentration. A plot of  $k_2$  vs  $[\text{H}_2\text{O}_2]$  is linear, but with a significantly large, positive intercept. The dependence of  $k_2$  on these reagents can be described by a mechanism in which cyclization of **C** to form a high-energy intermediate, **E**, competes with the base-catalyzed substitution of an additional molecule of hydrogen peroxide to form species **D** of Scheme 1.

We propose that cyclization of **C** to form imidazolylhydroxydioxetanone, **E**, is the primary reaction leading to chemiluminescence under excess  $\text{H}_2\text{O}_2$  conditions with an estimated unimolecular rate constant of  $0.14 \text{ s}^{-1}$ , derived from the intercept of the plot of  $k_2$  versus hydrogen peroxide concentration. Stevani et al. and Hohman et al. have demonstrated that aryl monoperoxyoxalates, similar to **C**, are stable in the presence of a fluorophor, but addition of a base leads to rapid chemiluminescence.<sup>28,29</sup> Using sodium salicylate, a stronger base than imidazole, the conversion of **C** to a high-energy intermediate is nearly 1 order of magnitude faster, whereas the formation rate is nearly 1 order of magnitude slower. This result is consistent with nucleophilic catalysis for the first substitution of hydrogen peroxide and cyclization of the peroxyoxalate product, leading to the phenol-substituted hydroxydioxetanone analogue of **E** (structure II of the Introduction), as first suggested by Catherall et al.<sup>5</sup> This structure is analogous to dioxetanones that have been shown to produce the singlet excited state of fluorescent acceptor molecules in a

(21) Bruice, T. C.; Schmir, G. L. *J. Am. Chem. Soc.* **1957**, *79*, 1663–1667.

(22) Kirsch, J. F.; Jencks, W. P. *J. Am. Chem. Soc.* **1964**, *86*, 833–837.

(23) Kirsch, J. F.; Jencks, W. P. *J. Am. Chem. Soc.* **1964**, *86*, 837.

(24) Menger, F. M.; Vitale, A. C. *J. Am. Chem. Soc.* **1973**, *95*, 4931.

(25) Satterthwait, A. C.; Jencks, W. P. *J. Am. Chem. Soc.* **1974**, *96*, 7018–7031.

(26) Neuvonen, H. *J. Chem. Soc., Perkin Trans. 2* **1995**, 951.

(27) Orosz, G. *Tetrahedron* **1989**, *45*, 3493–3506.

(28) Stevani, C. V.; Campos, I. P. d. A.; Baader, W. J. *J. Chem. Soc., Perkin Trans. 2* **1996**, 1645–1648.

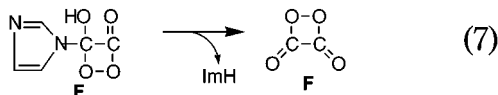
(29) Hohman, J. R.; Givens, R. S.; Orosz, G. *Tetrahedron Lett.* **1996**, *37*, 8273.

**Table 8.** Summary of Proposed Reaction Mechanism and Approximate Rate Laws

reaction step	excess H <sub>2</sub> O <sub>2</sub>	excess TCPO
TCPO + 2ImH → <b>B</b> + 2ArOH	rate = $k_1[\text{TCPO}][\text{ImH}]^2$ $K_1 = K_{\text{fall}}$	rate = $k_1[\text{TCPO}][\text{ImH}]^2$ $K_1 = K_{\text{rise}}$
<b>B</b> + H <sub>2</sub> O <sub>2</sub> → <b>C</b> + ImH	fast except for [H <sub>2</sub> O <sub>2</sub> ] < 5.0 mM	rate = $k_2[\text{B}][\text{ImH}][\text{H}_2\text{O}_2]$ $K_2 = K_{\text{fall}}$
<b>C</b> + H <sub>2</sub> O <sub>2</sub> → <b>D</b> + ImH	rate = $k_{2x}[\text{C}][\text{ImH}][\text{H}_2\text{O}_2]$ $k_{2x}$ obtained from slope of $k_{\text{rise}}$ vs [H <sub>2</sub> O <sub>2</sub> ]	slow, not probed by kinetics
<b>C</b> → <b>E</b>	rate = $k_{2y}[\text{C}][\text{ImH}]$ $k_{2y}$ obtained from intercept of $k_{\text{rise}}$ vs [H <sub>2</sub> O <sub>2</sub> ]	fast, not probed by kinetics
<b>E</b> + <b>F</b> → <i>hν</i> + products	fast compared to $k_1$ and $K_2$	fast compared to $K_1$ and $K_2$
<b>E</b> + ImH → non-CL products	faster than <b>E</b> + <b>F</b> and accounts for decreasing quantum yield with increasing [ImH]	faster than <b>E</b> + <b>F</b> and accounts for decreasing quantum yield with increasing [ImH]

chemically initiated electron-exchange luminescence (CIEEL) reaction.<sup>30–32</sup>

It is possible that the substituted dioxetanone, **E**, will release imidazole to form 1,2-dioxetanedione. This reaction may be catalyzed by proton addition to N-3 of the substituted imidazole from another molecule of imidazole and collapse of the tetrahedral intermediate.



Bifunctional catalysis by imidazole is well known,<sup>33,34</sup> and ester aminolysis reactions in aprotic solvents are accelerated by general acid catalysis.<sup>24</sup> In the case of 3-imidazolyl-3-hydroxydioxetanone, imidazole is an excellent electron-withdrawing leaving group, suggesting that the lifetime of **E** is short.

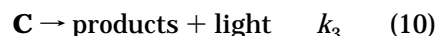
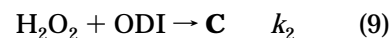
Obviously, an unambiguous assignment of the structure of the reactive intermediate that leads to chemiluminescence cannot be made from analysis of the reaction kinetics alone. Recently, Stevani et al. examined the imidazole-catalyzed PO-CL reaction and, on the basis of previous work with unstable four-membered cyclic peroxides, quantum yields of other dioxetanes, and the short-lived interconversion reactions of carboxylic acids with good leaving groups, proposed 1,2-dioxetanedione (**F**) as the most likely intermediate in peroxyoxalate chemiluminescence.<sup>10</sup> Although the results presented in this study are unable to distinguish between these two intermediates, we favor **E** because of the significant decrease in the quantum yield of the reaction with added imidazole. That imidazole decreases the quantum yield of the reaction suggests that deprotonation and formation of dioxetanedione (or two molecules of CO<sub>2</sub> directly) may be the main cause of signal reduction in the PO-CL reaction.

Base-catalyzed addition of hydrogen peroxide to imidazolyl hydroperoxide, **D**, apparently competes with formation of **E** and at high H<sub>2</sub>O<sub>2</sub> concentration and may also reduce the quantum yield of the reaction. The addition of hydrogen peroxide to imidazolyl hydroperoxyoxalate forming dihydroperoxyoxalate, species **D** in Scheme 1, has a complex dependence on the imidazole

concentration. As the imidazole concentration was increased,  $k_2$  increased linearly at low imidazole concentration but reached a maximum above 15 mM ImH. This dependence on the imidazole concentration can be explained by a two-step reaction in which hydrogen peroxide addition becomes rate-limiting. A similar maximum pseudo-first-order rate constant was observed in the imidazole-catalyzed reaction of ODI with hydrogen peroxide in acetonitrile, and the quantum yield decreased linearly with increasing H<sub>2</sub>O<sub>2</sub> concentration.<sup>19</sup> In contrast, in this work only a small reduction of the quantum yield was observed beyond 10 mM H<sub>2</sub>O<sub>2</sub>, suggesting that in ethyl acetate **D** might also cyclize to produce an energy-transfer intermediate.

**Excess TCPO Conditions.** Under conditions of [ImH] ≫ [TCPO] ≫ [H<sub>2</sub>O<sub>2</sub>],  $K_1$  has a second-order dependence on the imidazole concentration, with a termolecular rate constant of  $1.1(\pm 0.2) \times 10^2 \text{ M}^{-2} \text{ s}^{-1}$ . The nearly identical rate constant and same dependence on imidazole concentration strongly suggests that the initial reaction step is similar to what occurs under excess H<sub>2</sub>O<sub>2</sub> conditions. However, in this case the excess reagent, TCPO (0.075–0.25 mM), is 1–2 orders of magnitude less than the concentration of H<sub>2</sub>O<sub>2</sub> (2.5–15 mM) under excess H<sub>2</sub>O<sub>2</sub> conditions. As a result, the data suggest that reaction of H<sub>2</sub>O<sub>2</sub> with ODI to form the imidazolyl peracid (**C**) is sufficiently slow to correspond to the decline of the chemiluminescence signal. The first-order dependence of  $K_2$  on the initial TCPO concentration is readily explained by the reaction of H<sub>2</sub>O<sub>2</sub> with ODI derived from TCPO. Since loss reactions of **C** are fast compared to its formation, the kinetics under excess TCPO conditions provides no information about subsequent reactions of **C**. Those reactions are explored in another paper,<sup>19</sup> however, where the starting reagent is ODI rather than TCPO.

Although useful as a diagnostic, rise-fall kinetics as described by eqs 1 and 2 does not apply exactly to the proposed mechanism in which excess reagent TCPO is converted to ODI and followed by a pseudo-first-order reaction of H<sub>2</sub>O<sub>2</sub>. The appropriate integrated rate equations may be derived for the following mechanism:



Under conditions of [ImH] ≫ [TCPO] ≫ [H<sub>2</sub>O<sub>2</sub>], and reaction 9 slow compared to reaction 8, the ODI concen-

(30) Adam, W.; Liu, J.-C. *J. Am. Chem. Soc.* **1972**, *94*, 2894–2895.

(31) McCapra, F. *Prog. Org. Chem.* **1973**, *8*, 231.

(32) Schuster, G. B.; Horn, K. A. In *Chemical and Biological Generation of Excited States*; Academic Press: New York, 1982; pp 229–247.

(33) Bender, M. L.; Bergeron, R. J.; Komiyama, M. *The Bioorganic Chemistry of Enzyme Catalysis*; Wiley-Interscience: New York, 1984.

(34) Seoud, O. A. E.; Menegheli, P.; Pires, P. A. R.; Kiyani, N. Z. *J. Phys. Org. Chem.* **1994**, *7*, 431–436.

tration is given by

$$[\text{ODI}] = (1 - e^{-k_1 t})[\text{TCPO}]_0 \quad (11)$$

where  $k_1$  is the pseudo-first-order rate constant for a given imidazole concentration. The differential rate law for  $[\text{H}_2\text{O}_2]$  is

$$\frac{d[\text{H}_2\text{O}_2]}{dt} = -k_2[\text{H}_2\text{O}_2][\text{ODI}] = -k_2(1 - e^{-k_1 t})[\text{TCPO}]_0 [\text{H}_2\text{O}_2] \quad (12)$$

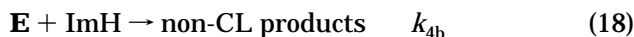
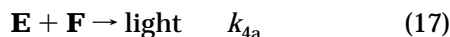
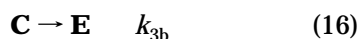
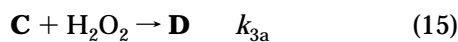
Rearranging and integrating gives a complex time dependence for  $\text{H}_2\text{O}_2$  concentration,

$$[\text{H}_2\text{O}_2] = [\text{H}_2\text{O}_2]_0 e^{-k_2[\text{TCPO}]_0 t} e^{-(k_2/k_1)e^{-k_1 t}[\text{TCPO}]_0} \quad (13)$$

If the reaction of **C** to form products is fast compared to its formation, we can assume steady state for **C** and calculate **C** from the above expressions for  $[\text{ODI}]$  and  $[\text{H}_2\text{O}_2]$

$$[\text{C}]_{\text{ss}} = \frac{k_2}{k_3} [\text{H}_2\text{O}_2][\text{ODI}] \quad (14)$$

The chemiluminescence signal is then proportional to  $[\text{C}]_{\text{ss}}$ . In the limit of the conversion of TCPO to ODI being fast in comparison to the reaction of  $\text{H}_2\text{O}_2$  with ODI, the above kinetics expressions simplify to describe simple rise-fall kinetics with  $k_1$  corresponding to the formation of ODI and  $k_2$  to the reaction of  $\text{H}_2\text{O}_2$  with ODI to form **C**. The effect of ImH on the quantum yield (profile area) can be accounted for by the reactions



where F is the fluorophor. Assuming that **D** is not an

energy-transfer intermediate as well, the chemiluminescence quantum yield is given by

$$\phi = \left( \frac{k_{4a}[\text{F}]}{k_{4a}[\text{F}] + k_{4b}[\text{ImH}]} \right) \left( \frac{k_{3b}}{k_{3b} + k_{3a}[\text{H}_2\text{O}_2]} \right) \quad (19)$$

Light emission from the peroxyoxalate chemiluminescence reaction is known to be linear over several orders of magnitude change in fluorophor concentration, requiring that  $k_{4b}[\text{ImH}] \gg k_{4a}[\text{F}]$ , and thus, the quantum yield is predicted to vary inversely with  $[\text{ImH}]$ , as is observed. If **D** also cyclizes to form an energy transfer intermediate, ImH could react with that species as well, again reducing the quantum yield of the reaction. This model provides a good description of the effects of all reagents on the chemiluminescence profile shapes and areas obtained under conditions of excess ODI concentration.

## Conclusions

Over a very wide range of reaction conditions, the kinetics of the imidazole-catalyzed peroxyoxalate reaction is consistent with the first step of the reaction being conversion of TCPO to ODI and the second step being the reaction of  $\text{H}_2\text{O}_2$  with ODI to form the imidazolyl peracid, **C**. Under conditions of excess  $\text{H}_2\text{O}_2$ , intermediate **C** may either cyclize in a unimolecular reaction to form a high-energy intermediate, **E**, or react with an additional molecule of  $\text{H}_2\text{O}_2$  to form **D**. Imidazole catalyzes all reaction steps with reaction orders consistent with this mechanism. Imidazole also decreases the quantum yield of the reaction. This negative effect on the chemiluminescence efficiency could be accounted for by catalysis of the decomposition of **C** to form nonlight producing products, possibly including 1,2-dioxetanedione, a postulated species long believed to be the key energy-transfer intermediate in the reaction.

**Acknowledgment.** The authors thank Shelley Copley for helpful discussions. The stopped-flow instrument was purchased under NSF Grant No. BIR-9302748.

JO9722109